Supporting Information to "Seasonal variation of nitryl chloride and its relation to gas-phase precursors during the JULIAC campaign in Germany"

Zhaofeng Tan[1], Hendrik Fuchs[1], Andreas Hofzumahaus[1], William J. Bloss[3], Birger Bohn[1], Changmin Cho[1], Thorsten Hohaus[1], Frank Holland[1], Chandrakiran Lakshmisha[1], Lu Liu[1], Paul S. Monks[2], Anna Novelli[1], Doreen Niether, Franz Rohrer[1], Ralf Tillmann[1], Thalassa Valkenburg[2], Vaishali Vardhan[1,a], Astrid Kiendler-Scharr[1], Andreas Wahner[1], Roberto Sommariva[2,3]

[1] Institute of Energy and Climate Research, IEK-8: Troposphere, Forschungszentrum Jülich GmbH, Jülich, Germany

[2] School of Chemistry, University of Leicester, Leicester, UK

[3] School of Geography, Earth and Environmental Sciences, University of Birmingham, Birmingham, UK

[a] now at, Department of Chemistry, University College Cork, Ireland

Correspondence: Zhaofeng Tan (zh.tan@fz-juelich.de) and Roberto Sommariva (rs445@le.ac.uk)

Table S1. Median, interquartile range (25%-75% percentiles) and maximum concentrations of 15-min averaged $ClNO_2$, NO_2 and O_3 concentrations during nighttime ($j_{NO3} < 1\times10^{-4}$ s^{-1}) in the different measurement periods of the JULIAC campaign.

		31 Jan – 8 Feb	4 – 31 Aug	9 – 30 Sep	1 – 25 Nov	1 – 31 Dec
	Median	150	22	45	46	80
$ClNO_2$ / pptv	25% – 75%	76 – 300	7 – 99	7 – 156	15 – 110	38 – 160
	Maximum	950	1410	1600	450	630
	Median	0.13	0.20	0.35	0.18	N.A.
NO / ppbv	25% – 75%	0.01 – 1.2	0.04 – 0.68	0.03 – 0.93	0.02 – 1.4	N.A.
	Maximum	33	6.4	12	19	N. A.
	Median	7.6	3.9	4.2	7.8	5.2
NO_2 / ppbv	25% – 75%	3.7 – 13	2.2 – 6.2	2.6 – 6.9	4.2 – 12.0	2.9 – 8.5
	Maximum	29	27	26	29	25
	Median	25	36	27	16	25
O_3 / ppbv	25% – 75%	17 – 32	27 – 48	22 – 33	9 – 24	15 – 31
	Maximum	38	100	64	36	42
	Median	4.4	20.8	16.7	8.0	8.4
T / °C	25% – 75%	2.1 –7.4	18 – 24	15 – 19	6 – 11	5 – 11
	Maximum	12	34	29	19	19
	Median	71	49	72	88	86
RH / %	25% – 75%	59 – 79	27 – 65	55 – 88	81 – 93	76 – 92
	Maximum	86	82	100	100	100

Table S2. Aerosol composition measured by AMS during the intensive measurement periods of the JULIAC campaign.

Group		PM_1 µg/m3	NO_3 µg/m3	SO_4 µg/m3	NH_4 µg/m3	Cl µg/m3	Organic µg/m3
Feb	Regional	0.97	0.24	0.10	0.09	0.01	0.53
	Long-Range	0.17	0.10	0.11	0.11	0.13	0.26
Aug	Regional	11.59	0.51	2.93	1.18	0.02	6.96
	Long-Range	3.83	0.20	1.03	0.41	0.01	2.17
Nov	Regional	4.63	1.09	0.76	0.50	0.05	2.23
	Long-Range	0.88	0.09	0.15	0.06	0.02	0.55

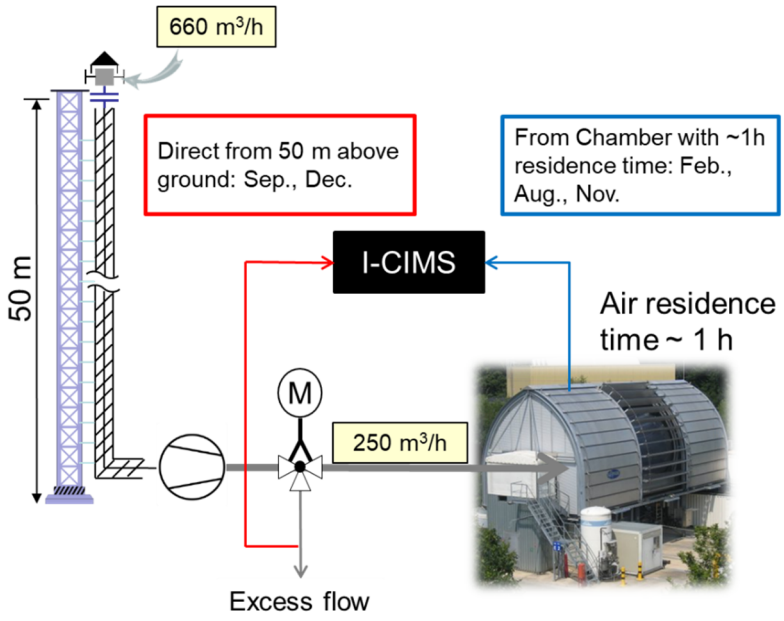

Figure S1. Schematic of the experimental setup of the JULIAC-SAPHIR system indicating the sampling points for the $ClNO_2$ measurements. During the intensive measurement periods of the JULIAC campaign (February, August, November), the I-CIMS instrument sampled from the SAPHIR chamber (blue line). Between the intensive measurement periods of the JULIAC campaign (September, December), the I-CIMS instrument sampled directly from the JULIAC tower (red line).

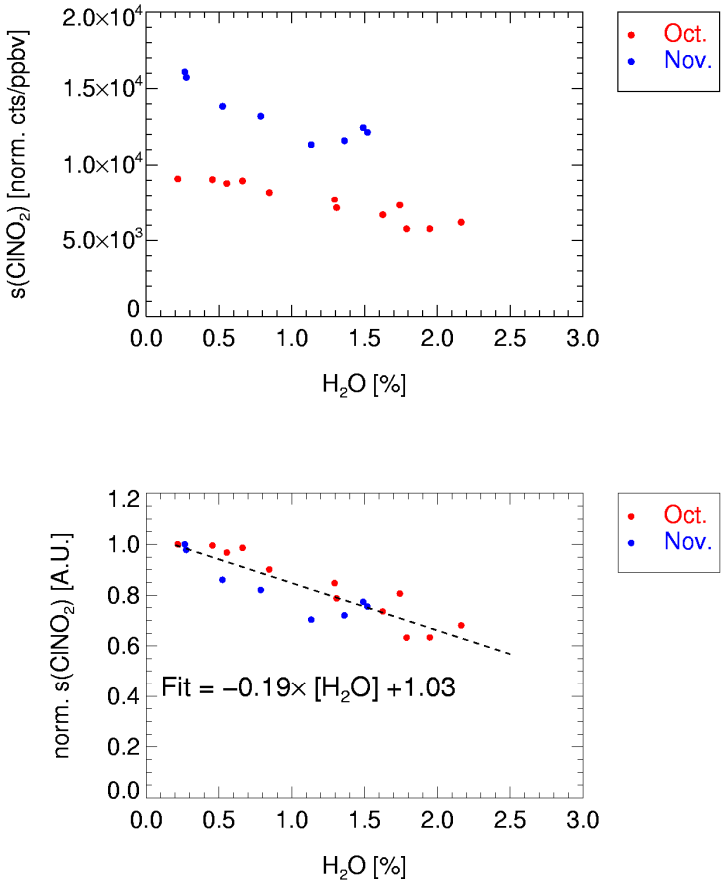

Figure S2. I-CIMS sensitivity dependence on the water vapor content determined in October and November during the JULIAC campaign. In calibration experiments, the inlet was overflowed with air containing a constant concentration of $ClNO_2$ (~5 ppbv) while varying the humidity. Upper panel: $ClNO_2$ signal (208 amu) normalized to the $(I\cdot(H_2O)^-)$ signal (145 amu) versus the H_2O mixing ratio by volume. Lower panel: Signals normalized to the maximum ClNO2 signal ($s(ClNO_2)/s(ClNO_2)_{max}$). A linear fit is used to derive the humidity dependence giving a decrease in the instrument sensitivity of 19% per 1% H_2O concentration.

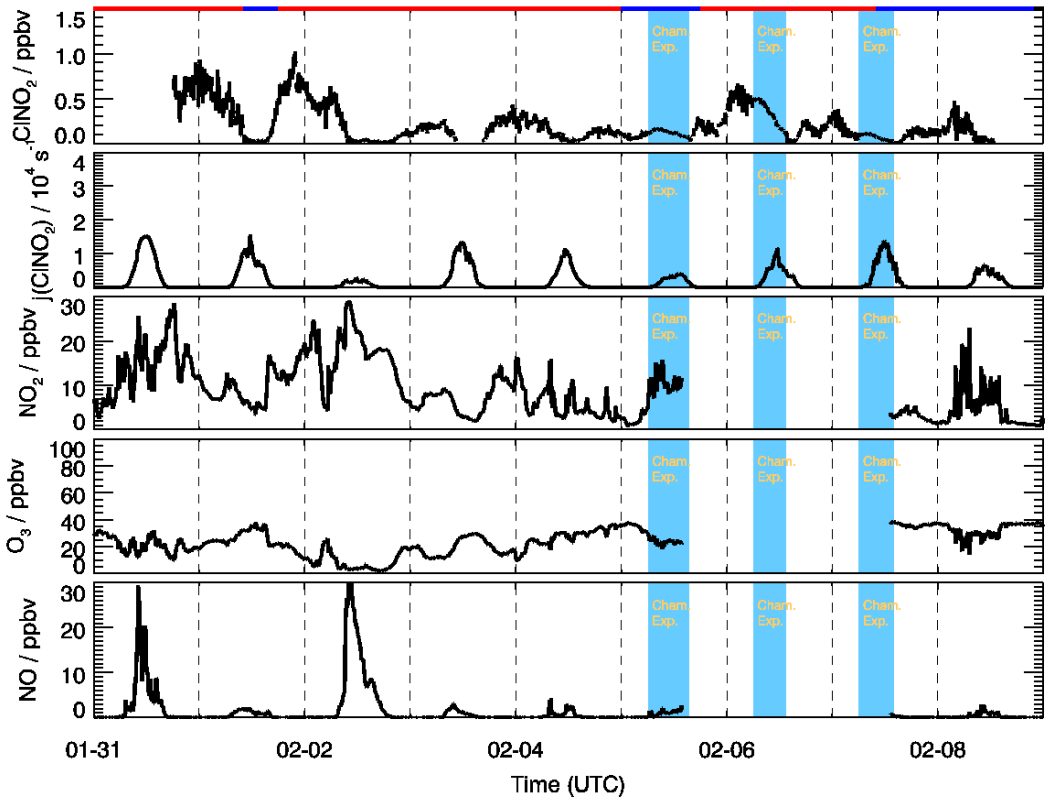

Figure S3. Time series of photolysis frequency $j(ClNO_2)$, $ClNO_2$, NO_2, O_3, and NO concentrations in February of the JULIAC campaign. Horizontal blue and red lines indicate air mass from long-range (blue) and regional transportation (red), respectively (Section 3.2). The color filled areas indicate periods when characterization experiments were performed: these measurements were excluded from the analysis.

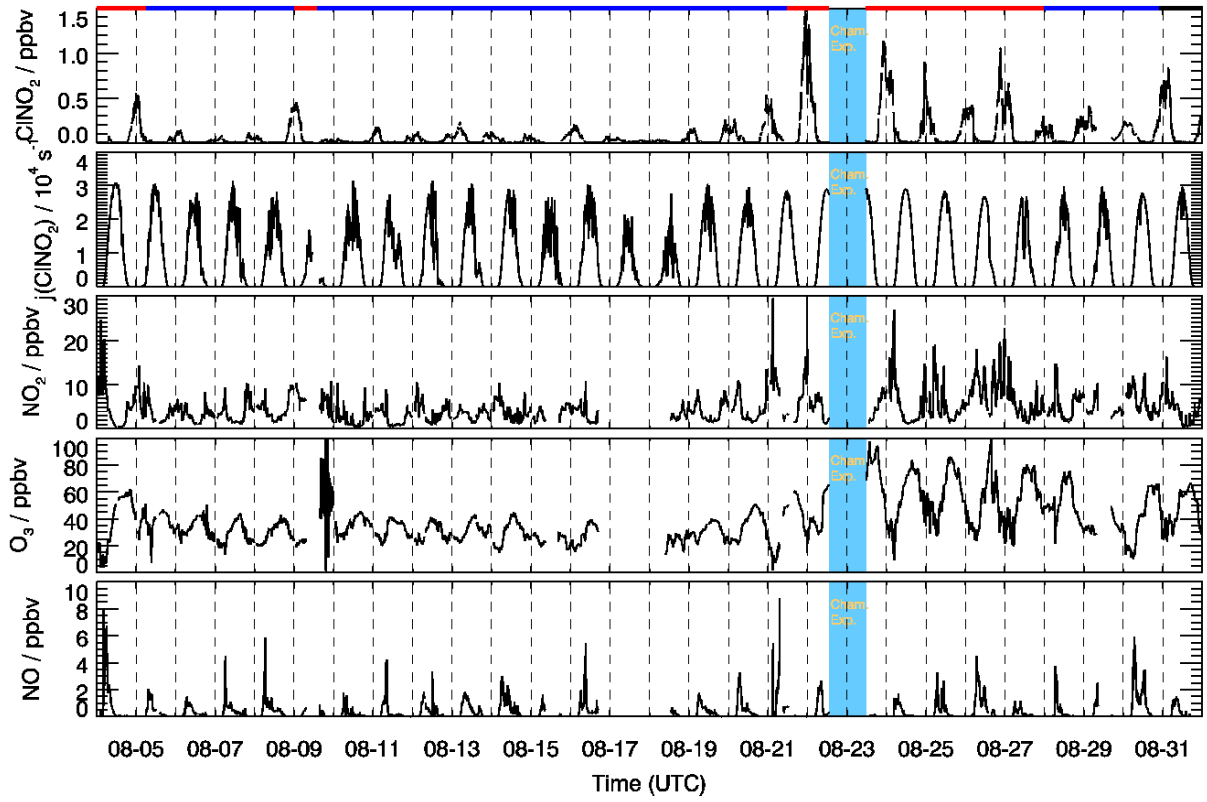

Figure S4. Same as Figure S3 but for the measurements in August.

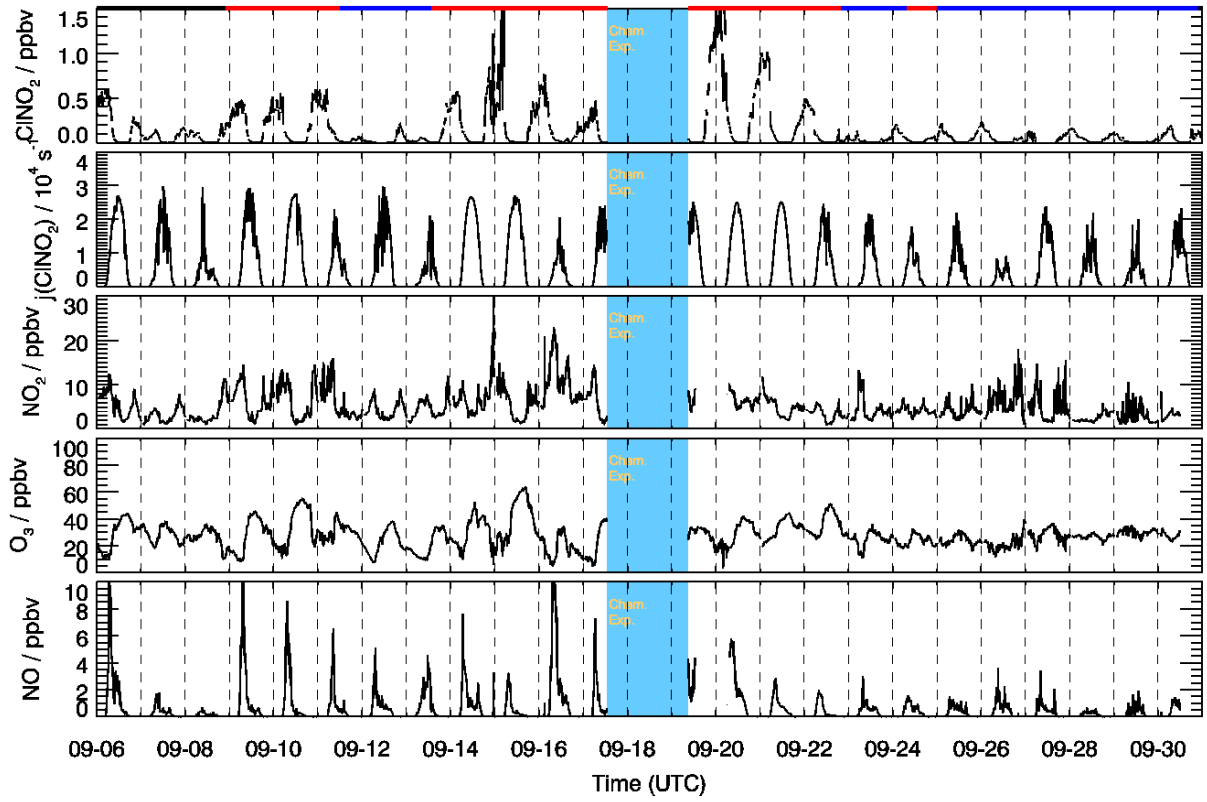

Figure S5. Same as Figure S3 but for the measurements in September.

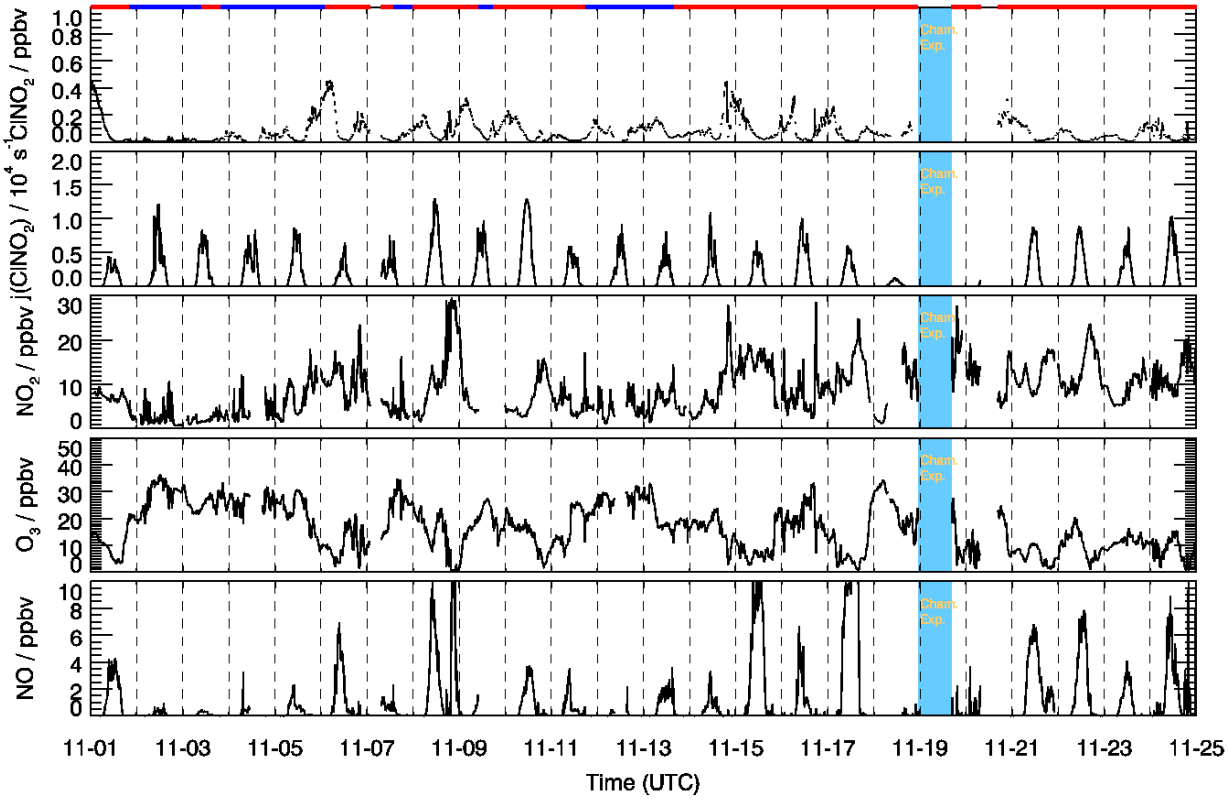

Figure S6. Same as Figure S3 but for the measurements in November.

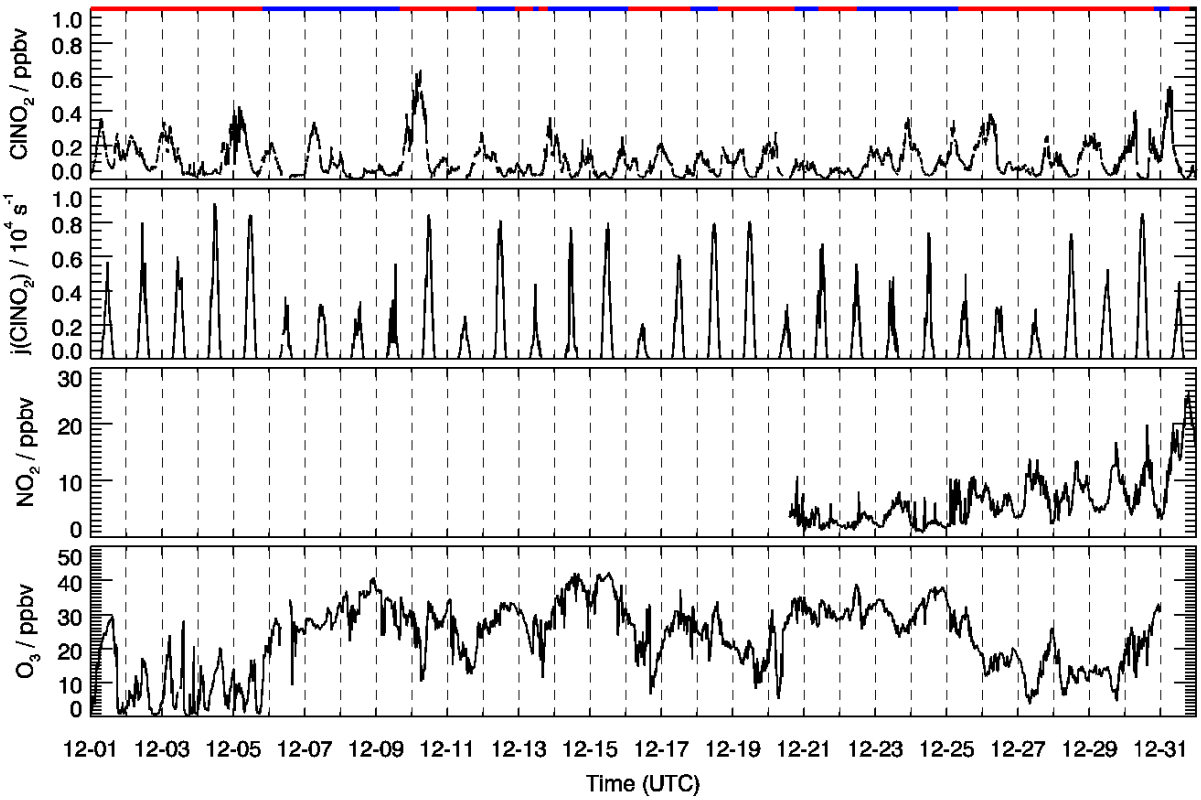

Figure S7. Same as Figure S3 but for the measurements in December. During this period NO measurements were not available.

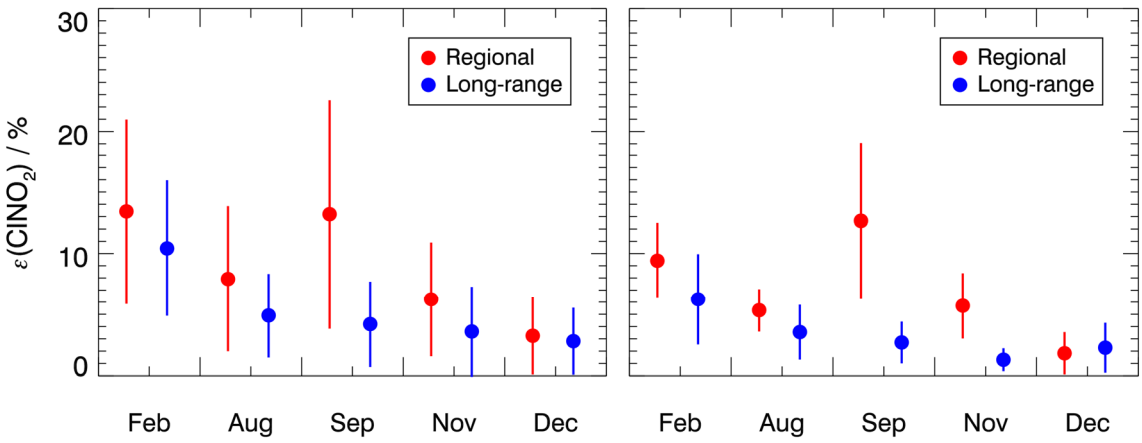

Figure S8. Same as Fig. 5 but for all nighttime data (left) and for data 1 hour (+/- 0.5h interval) before sunrise (right).

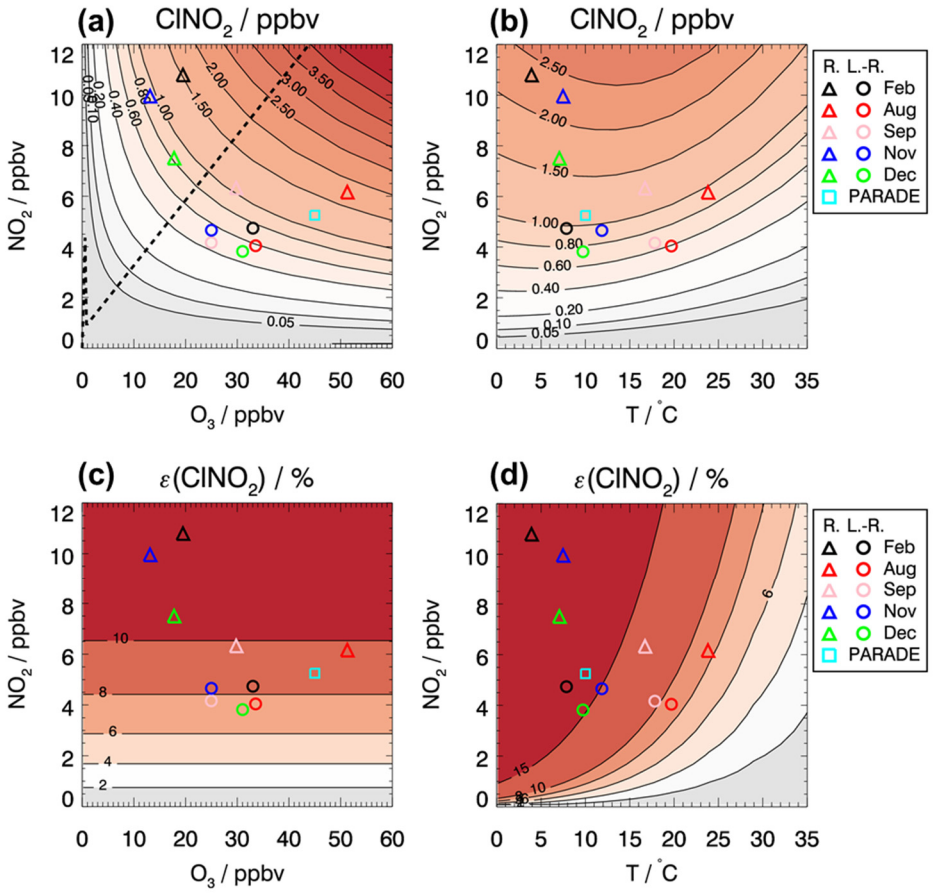

Figure S9. Same as Fig. 6 but the NO_3 radical chemical loss rate constant is decreased from 0.001 s^{-1} to 0.0005 s^{-1}.

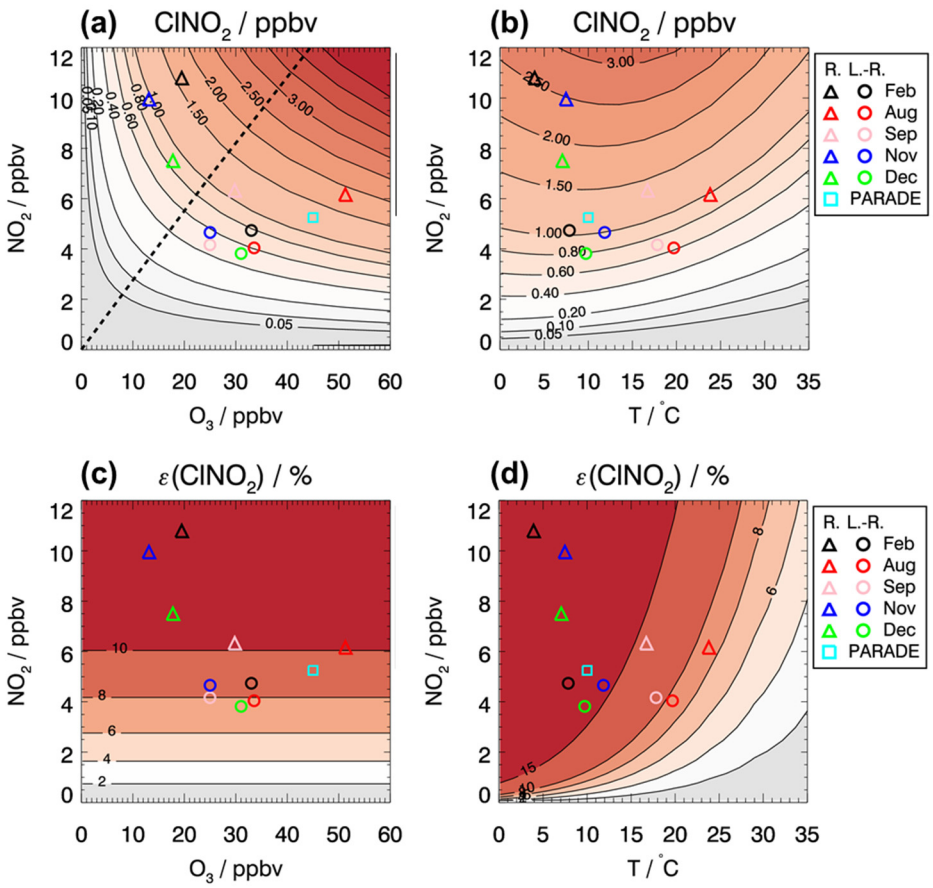

Figure S10. Same as Fig. 6 but the N_2O_5 heterogeneous uptake coefficient on aerosol is increased from 0.01 to 0.02.

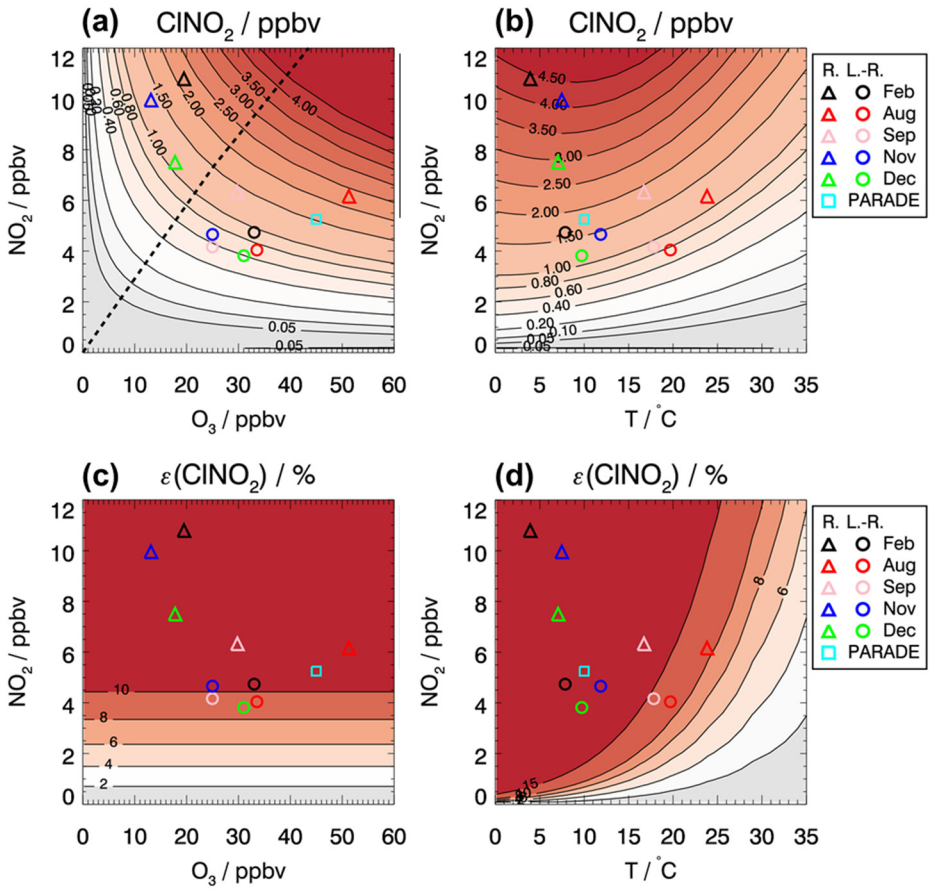

Figure S11. Same as Fig. 6 but the yield of $ClNO_2$ in the heterogeneous reaction of N_2O_5 on aerosol is increased from 0.5 to 1.0.